Extended x-ray absorption fine structure and molecular dynamics simulation studies on the structure of CuX- and AgX-based glasses (X = Cl, Br and I)

Extended x-ray absorption fine structure and molecular dynamics simulation studies on the structure of CuX- and AgX-based glasses (X = Cl, Br and I)

Kohei Kadono†, Masanori Shojiya‡, Hiroyuki Kageyama§, Nagao Kamijo†, Yoji Kawamoto‡ and Hiroshi Tanaka†

† Department of Optical Materials, Osaka National Research Institute, AIST, Ikeda, Osaka 563-8577, Japan
‡ Division of Science of Materials, Graduate School of Science and Technology, Kobe University, Nada, Kobe 657-8501, Japan
§ Department of Material Physics, Osaka National Research Institute, AIST, Ikeda, Osaka 563-8577, Japan

Abstract. Extended x-ray absorption fine structure (EXAFS) spectra at the Cu K-edge and Ag K-edge were measured for copper(I) halide-based and silver halide-based glasses, respectively. Molecular dynamics (MD) simulation was also performed for the glasses with the same compositions. The bond distances, A–X, in the copper(I) halide-based and the AgI-based glasses, which were obtained from the EXAFS analyses, were almost the same as those in the CuX (X = Cl, Br, I) and AgI crystals. The coordination numbers of halide ions around the monovalent metal ions were nearly four as well as those in the crystals. These results were consistent with those of the MD simulation. On the other hand, the EXAFS analyses showed that the bond distances in the AgCl-based and the AgBr-based glasses were 0.1 Å shorter than those in the AgCl and AgBr crystals. These values are in the range of those of the halogenoargentate crystals having three- or fourfold coordination. However, the coordination numbers obtained from the EXAFS analyses were larger than four. The MD simulation suggested that the coordination shells in the AgCl-based and the AgBr-based glasses are highly disordered.

1. Introduction

The discovery of the fluorozirconate glass system [1] and the subsequent research on the peculiar structure and the properties of these glasses [2] stimulated the exploration of new glass families based on not only fluoride but also other halides, i.e., chlorides, bromides and iodides [3]. We have also reported new glass-forming systems based on AX_n–MX–$M'X_2$ where A = Zn, Cd $(n = 2)$, A = Li, Cu, Ag $(n = 1)$, M = K and/or Cs, M′ = alkaline earth elements (Ca, Ba) and X = Cl, Br, I [4, 5]. Among the components of these systems, AX_n are regarded as glass-forming halides, although most of the AX_n are not vitrified without the addition of other halides. Structural analyses have been performed for the glasses based on zinc and cadmium halides [4, 6]. The studies have revealed that the zinc halide-based and the CdI_2-based glasses are composed of corner-shared ZnX_4 and CdI_4 tetrahedra, whereas the $CdCl_2$-based glass has a local structure of sixfold Cl coordination of Cd. The network structure of the zinc halide-based and the CdI_2-based glasses may be consistently described by a continuous random network model as well as typical oxide glasses and a

single component $ZnCl_2$ glass [7]. On the other hand, the structure of the $CdCl_2$-based glass is approximately described by a random close-packed structure model which has been proposed for fluorozirconate glasses. Therefore, it is of interest to investigate the structural characteristics of the glasses based on the monovalent metal halides, AX where A = Li, Cu and Ag.

The glass systems based on the monovalent metal halides are characterized by the following properties. The glasses have low glass transition temperatures, i.e., from less than room temperature for the AgCl-based and the AgBr-based glasses to about $70\,°C$ for the lithium halide-based glasses [5]. The glasses are transparent in the visible to the far-infrared region; the cut-off wavelengths in the infrared region are in the range of about 10 μm for the LiCl-based glass to about 30 μm for the AgI-based glass [5]. The glasses have high ionic conductivity at room temperature, i.e., from 10^{-8} S cm^{-2} for the LiCl-based glass to 10^{-3} S cm^{-2} for the AgI-based glass [8]. The glass-forming regions in these systems are extremely limited; the systems are vitrified by a conventional melt-quenching method in the compositional regions of AX = 50 to 60 mol%, MX = 40 to 50 mol% and $M'X_2 = 0$ to 25 mol%. However, it is noteworthy that the molar ratio of halide ions to the glass-forming cations, A^+, is around 2 for the glass-forming compositions. Phenomenologically, this can be interpreted as follows. In phase diagrams of AX–MX (M = alkali elements), eutectic points are observed at 50 mol% of AX and 50 mol% of MX, so that the liquidus temperature will become the lowest in this molar ratio region. Thus the viscosities of the melts are expected to be large and the melts will be easily vitrified by the addition of the third additives, $M'X_2$ [5].

When the glasses are obtained by a melt-quenching method, the structural units of the glass network are expected to be similar to those of the crystals and/or the molten salts of the glass-forming halides. The structures of lithium halides, AgCl and AgBr crystals are the NaCl type whereas copper(I) halides and AgI crystals have zinc-blende type structure [9]. In the former type of structure, cations are coordinated by six halide ions while the latter has fourfold coordination structure. Thus, the monovalent glass-forming cations have different local structures in their crystals. In crystals of halogenocuprate(I) and argentate, however, most of the polyhedra have fourfold or less than fourfold coordination. In molten states, on the other hand, conflicting results have been reported for lithium halides; one is fourfold coordination and the other is sixfold coordination [10]. It has been reported that copper(I) halides and silver halides have fourfold coordination in their molten salts [11]. In spite of the similarity in their macroscopic properties, therefore, one can expect some peculiarity and variety in the structures of the monovalent halide-based glasses.

The structural analysis on the lithium halide-based glasses have been carried out by means of neutron scattering [12] and molecular dynamics (MD) simulation [13]. It has been revealed that the coordination numbers around lithium ions are almost four. The MD simulation has showed that about 80% of the tetrahedral units are connected by corner sharing and the others, by edge sharing [13]. Therefore, the structure of the glasses substantially satisfies Zachariasen's glass-forming rule and may be described by a continuous random network model [14].

In this study we have performed structural analyses on the glasses based on copper(I) halides and silver halides by means of extended x-ray absorption fine structure spectroscopy (EXAFS) and molecular dynamics simulation. EXAFS spectroscopy is one of useful methods for observing the local structure. In particular, for multicomponent systems such as the monovalent-halide-based glasses, this technique is much more powerful because structural parameters surrounding a given atom can be extracted. The local structures around Cu^+ and Ag^+ ions are discussed on the basis of the coordination structures of

halogenocuprate(I) and halogenoargentate complexes and the results of the MD simulations on these glasses.

2. Experimental details

2.1. Preparation of glasses

Reagent grade anhydrous halides were used for preparation of the glasses. Since monovalent copper halides contained trace amounts of divalent impurities (Cu(II)), these were purified as follows. Copper(I) chloride and bromide were suspended in dilute hydrochloric and hydrobromic acid, respectively, and the Cu(II) impurities were dissolved. The CuCl or CuBr suspension were filtered and washed with ethanol. The powders of CuCl or CuBr were dried under vacuum and successively at about 250 °C. Copper(I) iodide was sublimated at about 500 °C under a reduced pressure. Alkali metal halides and alkaline-earth metal halides were used after vacuum drying at elevated temperatures. Silver halides were used without any purification.

Batch mixtures of the halides with total amounts of 3 to 4 g were melted in silica glass crucibles. The melts were quenched between two stainless plates. Since several glasses have glass transition temperatures lower than room temperature, the stainless plates were cooled at about −15 °C and the glasses were carefully kept at low temperatures. The obtained glasses were transparent. Since some of the starting halide compounds and the glasses are hydroscopic, all preparation procedures were carried out in a glove box filled with dry nitrogen or argon. The compositions of the glasses used for EXAFS measurements are summarized in table 1.

Table 1. Compositions (mol%) of the glasses for the EXAFS measurements.

Copper(I) halide-based glass	55 CuCl • 24 KCl • 6 CsCl • 15 $BaCl_2$
	55 CuBr • 24 KBr • 6 CsBr • 15 $BaBr_2$
	55 CuI • 24 RbI • 6 CsI • 15 BaI_2
Silver halide-based glass	55 AgCl • 20 KCl • 20 CsCl • 5 $BaCl_2$
	55 AgBr • 20 KBr • 20 CsBr • 5 $BaBr_2$
	55 AgI • 20 KI • 20 CsI • 5 BaI_2

2.2. EXAFS measurements

Powdered copper(I) halide-based glasses and flakelike silver halide-based glasses were sealed with polyethylene films for EXAFS measurements. During the measurements, we covered the silver halide-based glass samples with black sheets to avoid exposure of them to light. The measurements were performed at Beam Line 7C and 10B of the Photon Factory, the National Laboratory for High Energy Physics (KEK, Tsukuba). The positron energy and the ring current of the storage ring were 2.5 GeV and 200–360 mA, respectively. The monochromators with two flat Si(111) (BL7C) or channel-cut Si(311) (BL10B) were used. The incident beam intensity of the x-ray, I_0, and the transmitted beam intensity through samples, I, were monitored by ionization chambers with flowing gases of 100% N_2 and 85% $N_2 + 15%$ Ar or 100% N_2 at the Cu K-edge, and 50% $N_2 + 50%$ Ar and 100% Ar at the Ag K-edge, respectively.

2.3. Molecular dynamics simulation

Molecular dynamics simulations were performed for the NTP ensemble using an MXDORTO program [15]. Total numbers of ions were more than 400 and the number ratios of the ions were determined such that the compositions correspond to those of the glasses used for EXAFS measurements (table 1). Cubic simulation cells of 23^3–27^3 Å^3 depending on the glass compositions were used. The external pressure was set at 0.1 MPa. An interionic potential function of Busing–Ida–Gilbert type given by equation (1) was used,

$$U_{ij}(r_{ij}) = \frac{z_i z_j e^2}{r_{ij}} + f_0(b_i + b_j)\exp\left(\frac{a_i + a_j - r_{ij}}{b_i + b_j}\right) - \frac{c_i c_j}{r_{ij}^6} \tag{1}$$

where ze is the ionic charge, a, b and c are the potential parameters, r_{ij} is the interionic distance between ions i and j and f_0 ($=6.9472 \times 10^{-11}$ erg) is a constant for unit conversion between these terms. The Coulombic term of the potential function was calculated by using the Ewald method. The potential parameters were determined to give correct structures of reference crystals by performing molecular dynamics calculations. Table 2 shows the parameters of the respective ions. It was confirmed that these potential parameters successfully reproduce the densities and the bond distances close to those observed for several crystals.

Table 2. Potential parameters used for the MD simulation.

Ion	z	a (Å)	b (Å)	c (Å)
Cu$^+$	+1.0	0.945[a], 0.755[b]	0.080	0.000
Ag$^+$	+1.0	1.260[a], 1.005[b]	0.080	0.000
K$^+$	+1.0	1.595	0.080	0.000
Rb$^+$	+1.0	1.725	0.080	0.000
Cs$^+$	+1.0	1.915	0.080	0.000
Ba^{2+}	+2.0	1.735	0.080	0.000
Cl$^-$	−1.0	1.925	0.090	35.000
Br$^-$	−1.0	2.060	0.090	40.000
I$^-$	−1.0	2.265	0.090	50.000

[a] For chlorides and bromides.
[b] For iodides.

The glassy states were produced by the same procedure as the melt-quenching method in the laboratory. The details are as follows:

(1) The calculations were started from a randomly constructed initial configuration of ions. The systems were equilibrated at a temperature of 1000 K for 3000 steps with 1.0 to 1.5 fs interval and then for 25 000 steps with 2.5 fs interval.

(2) The systems were cooled from 1000 K to 600 K for 4000 steps with 4.0 fs interval. The cooling rate was 2.5×10^{13} K s^{-1}. After the cooling, the systems were equilibrated at 600 K for 15 000 steps with 4.0 fs interval.

(3) The temperatures of the systems were again decreased from 600 K to 300 K with the same cooling rate (3000 steps with 4.0 fs interval). Then an equilibration run for 15 000 steps with 4.0 fs interval was performed.

After establishing the glassy state, the structural data were accumulated during the equilibration run. The calculations for some glass systems were repeated several times starting from different initial configurations in order to estimate errors due to the variation

from run to run. The estimated errors were ± 0.02 Å and ± 0.2 for the bond distance and the coordination number, respectively.

3. Experimental results and data analyses

3.1. EXAFS

Analyses of EXAFS data were performed by using the programs by Sakane [16]. After the subtraction of a Victoreen-type base-line of the pre-edge region, EXAFS oscillations $\chi(k)$ were extracted using cubic spline functions. The $\chi(k)$ spectra of the Cu K-edge for the copper(I) halide-based glasses and the Ag K-edge for the silver halide-based glasses are shown in figures 1 and 2, respectively. These spectra are normalized with backscattering amplitudes of the respective scattering atoms. Fourier transformation was carried out for the normalized $\chi(k)$ spectra in the region of 4–10 Å^{-1} for the CuCl-based and AgCl-based
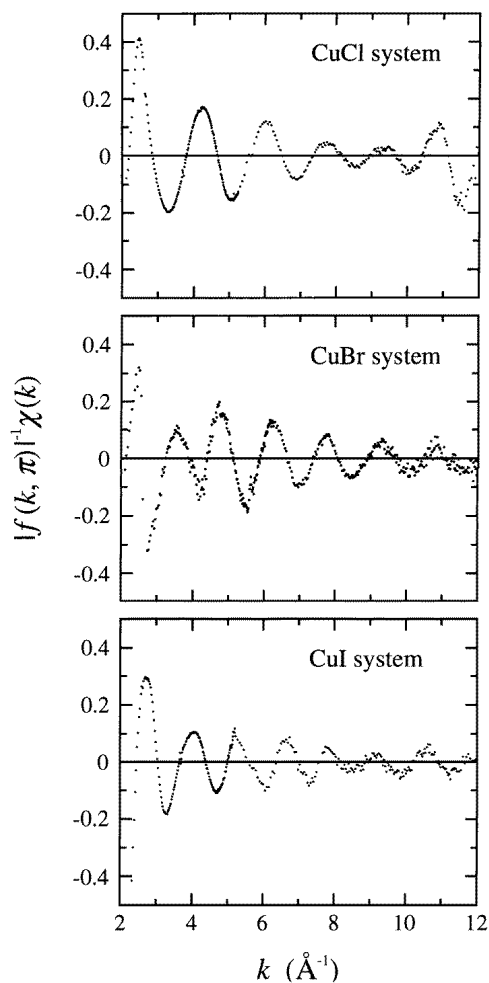
Figure 1. $\chi^{(3)}$ spectra of Cu K-edge for copper(I) halide-based glasses. The spectra are normalized with backscattering amplitudes of the respective scattering atoms.
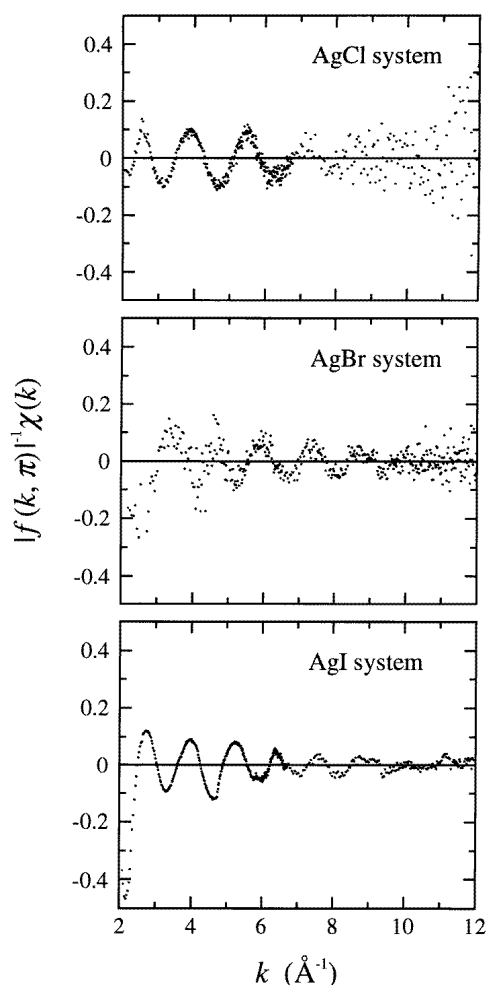
Figure 2. $\chi^{(3)}$ spectra of Ag K-edge for silver halide-based glasses. The spectra are normalized with backscattering amplitudes of the respective scattering atoms.

systems, 4–11 Å^{-1} for the CuBr- and CuI-based systems, 4.5–10.5 Å^{-1} for the AgBr-based system, and 5–11 Å^{-1} for the AgI-based system. Imaginary and absolute parts of the Fourier transforms are shown in figures 3 and 4. The prominent peaks of the absolute parts located at 2–3 Å are assigned to nearest neighbouring halide ions around Cu^+ or Ag^+ ions. These peaks are filtered in an appropriate region and inversely Fourier transformed into k-space. The least-squares fits in the k-space were carried out for the inversely Fourier transformed spectra using the single scattering EXAFS formula,

$$\chi(k) = \sum_j \frac{N_j}{R_j^2 k_j} |f_j(k_j)| \exp(-2\sigma_j^2 k_j^2) \exp(-2R_j/\lambda_j) \sin(2k_j R_j + \delta_j(k_j)) \tag{2}$$

where N_j, R_j, σ_j and λ_j are the coordination number, the bond distance, the Debye–Waller-type thermal parameter and the mean free path of the photoelectron of the jth coordination shell, respectively; $f_j(k)$ and $\delta_j(k)$ are the theoretically calculated backscattering amplitude
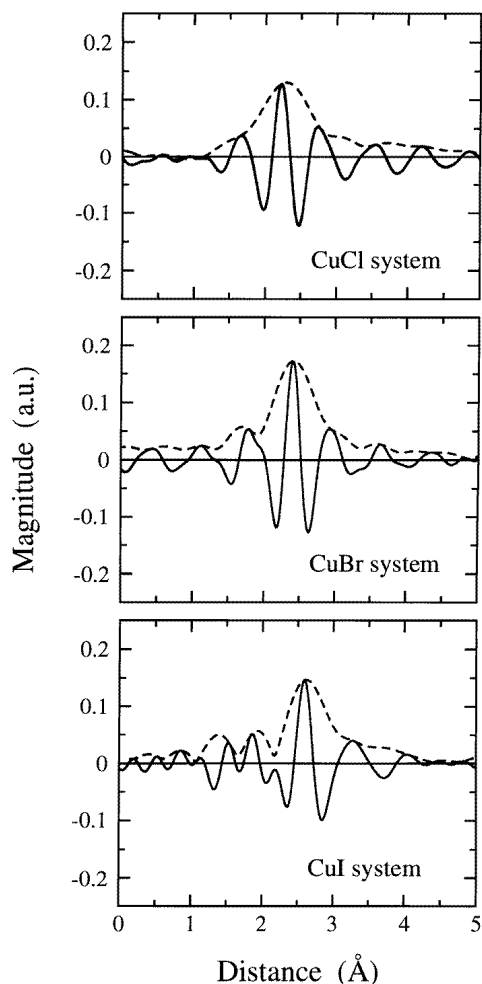
Figure 3. Imaginary and absolute parts of Fourier transforms of $\chi^{(3)}$ spectra of Cu K-edge for copper(I) halide-based glasses.

and total phase shift [17]. The photoelectron wave vectors k and k_j are defined by

$$k = (2m/h^2(E - E^{exp}))^{1/2} \tag{3}$$

and

$$k_j = (k^2 - 0.2625(\Delta E_j))^{1/2} \tag{4}$$

where m and h are the mass of the electron and the Planck constant, respectively; E and E^{exp} are the x-ray photon energy and the experimental threshold energy. The threshold energy was determined from 8979.23 eV to 8981.23 eV for Cu K-edge spectra and from 25 490.37 eV to 25 502.83 eV for Ag K-edge spectra. The ΔE_j is defined as the difference between the E^{exp} and the theoretical threshold energy.

The curve-fitting analyses were performed using the one-shell model with σ, λ and ΔE as variable parameters for crystals. For glasses, N, R and σ were used as variable
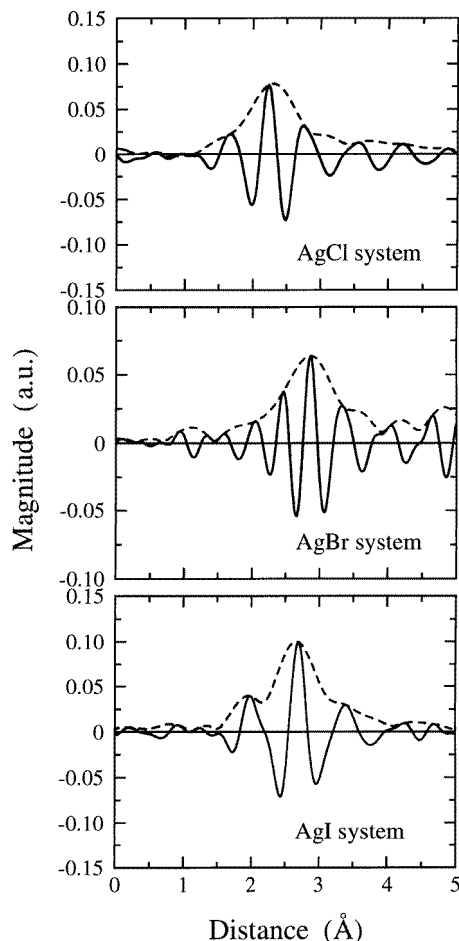
Figure 4. Imaginary and absolute parts of Fourier transforms of $\chi^{(3)}$ spectra of Ag K-edge for silver halide-based glasses.

parameters and ΔE and λ were kept fixed at the values determined in the curve-fitting of the corresponding crystals. Figures 5 and 6 show the inversely Fourier transformed spectra and the results of the least-squares curve fitting. Tables 3 and 4 present the structural parameters of the crystals and the glasses which were obtained by the curve-fitting. The experimental errors were estimated as about ± 30, ± 1 and $\pm 10\%$ for the coordination number, the bond distance and the Debye–Waller-type parameter, respectively. These values were determined as follows. The errors on the coordination number and the Debye–Waller-type parameter were estimated by varying λ or N for the crystals or the glasses, respectively, until the reliability factor (r-factor) increased to $2^{1/2}r_{min}$; r_{min} is the minimum value of the r-factor which is obtained at best fitting. For the bond distance, the error was estimated by varying ΔE until the r-factor increased to $2^{1/2}r_{min}$. This method takes account of the strong correlation between N or λ and σ, and between R and ΔE [18].
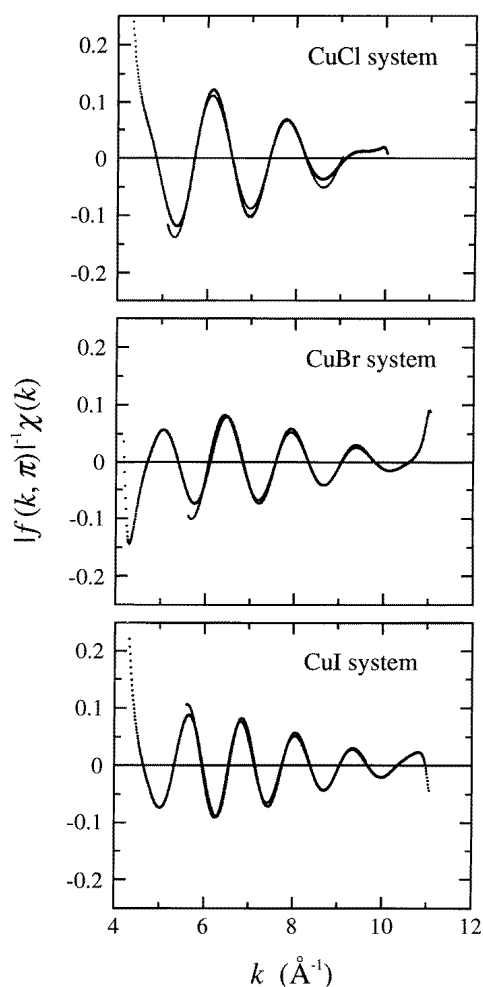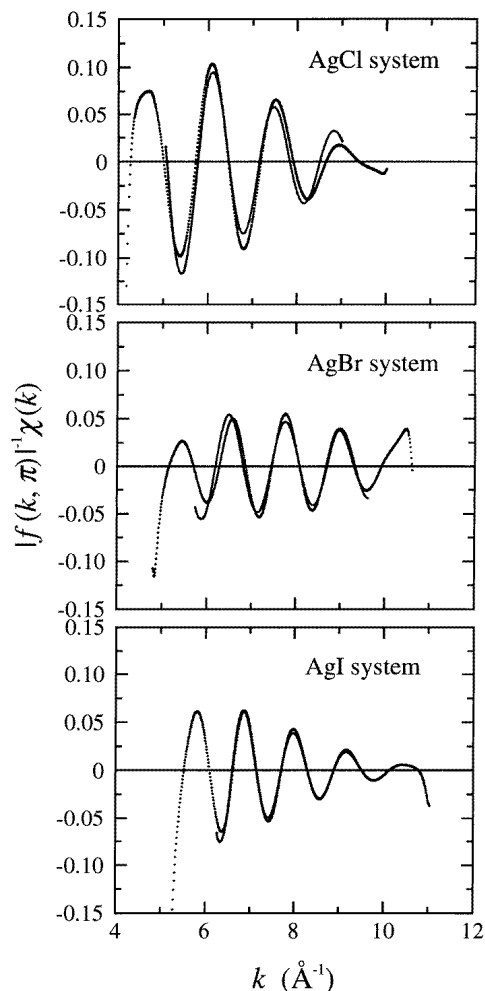
Figure 5. Inverse Fourier transforms (dotted lines) and least-squares curve fits (solid lines) for Cu K-edge for copper(I) halide-based glasses.

3.2. Molecular dynamics simulation

As an example, the internal energy of the CuBr-based system was plotted against the temperature in figure 7. The slope of this plot changes at about 600 K. This point is regarded as the glass transition temperature of the system. The temperature is higher than the glass transition temperature experimentally obtained for the real glass (about 300 K). This disagreement is due to the extremely large cooling rate in the simulation; the cooling rate in the melt-quenching method in laboratory experiment is usually 10^6–10^7 K s^{-1} which is 10^7 slower than those in the MD simulation. The observation of the glass transition temperature in the MD simulation indicates that the glassy state was successfully produced in this system.

Tables 5 and 6 present the results of the MD simulations; the average bond distances, the coordination numbers of halide ions around cations and the manner of linkage of the tetrahedral units in the copper(I) halide-based and silver halide-based glasses, respectively. The distribution of X–A–X angles in the glasses are shown in figures 8 and 9.

Figure 6. Inverse Fourier transforms (dotted lines) and least-squares curve fits (solid lines) for Cu K-edge for silver halide-based glasses.

4. Discussion

4.1. Copper(I) halide-based glasses

As seen from table 3, the coordination numbers of halide ions around Cu^+ in the copper(I) halide-based glasses obtained from EXAFS analyses were near four. The Cu–X bond distances in the glasses were 2.31, 2.46 and 2.63 Å for chloride, bromide and iodide, respectively. The bond distances were very close to those in the corresponding crystals, i.e., CuCl, CuBr and CuI, the structures of which are the zinc-blende type at room temperature.

In order to compare the coordination structure in the copper(I) halide-based glasses with those in crystals in more detail, we examine the relationship between the coordination structure and the bond distance in complex crystals containing halogenocuprate(I) polyhedra. In figure 10, the Cu–X bond distance of halogenocuprate(I) polyhedra in more than 50 complexes and CuX crystals are plotted against the coordination number [9, 19]. In all of

Table 3. Structural parameters of the copper(I) halide-based systems obtained by the EXAFS curve-fitting[a,b].

System		N	R (Å)	σ (Å)	λ (Å)	ΔE (eV)	r^c (%)
CuCl	crystal	(4)	(2.341)	0.083	3.78	−3.82	12.6
	glass	4.5	2.31	0.103	(3.78)	(−3.82)	14.2
CuBr	crystal	(4)	(2.464)	0.096	6.70	−4.11	9.9
	glass	4.0	2.46	0.102	(6.70)	(−4.11)	11.7
CuI	crystal	(4)	(2.617)	0.096	6.91	−3.75	9.3
	glass	3.1	2.63	0.104	(6.91)	(−3.75)	11.3

[a] Numerals in parentheses are fixed in curve-fitting process.
[b] Experimental errors were estimated as about ±30, ±1, ±10% for coordination numbers, bond distances and Debye–Waller-type parameters, respectively. (See the text section 3.1.)
[c] Reliability factor.

Table 4. Structural parameters of the silver halide-based systems obtained by the EXAFS curve-fitting[a,b].

System		N	R (Å)	σ (Å)	λ (Å)	ΔE (eV)	r^c (%)
AgCl	crystal	(6)	(2.774)	0.112	4.35	−1.74	14.8
	glass	6.1	2.66	0.115	(4.35)	(−1.74)	26.4
AgBr	crystal	(6)	(2.887)	0.076	2.31	−9.95	12.5
	glass	6.6	2.79	0.064	(2.31)	(−9.95)	21.4
AgI	crystal	(4)	(2.803)	0.103	6.43	−2.10	8.7
	glass	4.6	2.81	0.120	(6.43)	(−2.10)	9.8

[a] Numerals in parentheses are fixed in curve-fitting process.
[b] Experimental errors were estimated as about ±30, ±1, ±10% for coordination numbers, bond distances and Debye–Waller-type parameters, respectively. (See the text section 3.1.)
[c] Reliability factor.

the crystals, Cu^+ ions are located in coordination sites of fourfold or less than fourfold. The bond distances vary greatly with the coordination number; the bond distances increase with increasing coordination number. As seen from this figure, the Cu–X distances in the copper(I) halide-based glasses, which were obtained from EXAFS analyses, are in the range of threefold or fourfold coordination. This fact strongly supports that the coordination number in the CuX-based glasses are four as expected from the EXAFS analyses.

These results are consistent with the results of the MD simulation of copper(I) halide-based glasses in table 5, which shows that more than 70% of Cu^+ ions are coordinated by four halide ions in the glasses. As shown in figure 8, the distribution of the bond angle, X–Cu–X, of the fourfold coordination polyhedra has a peak at about 110°. This indicates that the fourfold coordination polyhedra have tetrahedral configuration. Most of the CuX_4 tetrahedra are connected by sharing the corners (see table 5). Thus, we conclude that the main structural unit of the copper(I) halide-based glasses is the corner-sharing CuX_4 tetrahedron. The structural characteristics of the copper(I) halide-based glasses substantially satisfy the Zachariasen's glass-formation rule for oxide glasses. However, it should be noted that more than 10% of the linkages of tetrahedra are edge sharing.
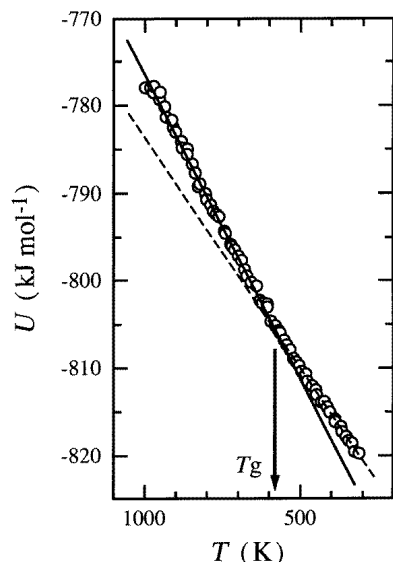
Figure 7. Temperature dependence of the internal energy of CuBr-based glass in the MD simulation.

Table 5. Coordination numbers around Cu^+ ion, manner of linkage of CuX_4 tetrahedra and Cu–X bond distances in the structure of CuX-based glasses simulated by the MD calculation.

| System	X^- coordination number around Cu^+ (%)					Manner of linkage of CuX_4 tetrahedron (%)		Bond distance (Å)
	3	4	5	6	Average[a]	Corner-sharing	Edge-sharing	
CuCl	2	84	13	1	4.1	87	13	2.30
CuBr	4	93	3	0	4.0	89	11	2.49
CuI	27	73	0	0	3.7	83	17	2.52

[a] Average coordination number.

4.2. Silver halide-based glasses

The results of EXAFS analyses for the silver halide-based glasses were more complicated compared with those of the copper(I) halide-based glasses. The coordination numbers of halide ions around Ag^+ were 6.1, 6.6 and 4.6 for chloride, bromide and iodide, respectively. Taking into account the experimental error, these values are near to the coordination number in the corresponding crystals; at room temperature AgCl and AgBr crystals have sixfold coordination (NaCl structure) and AgI has fourfold coordination (zinc-blende structure). The Ag–X bond distances in the glasses were 2.65 Å, 2.79 Å and 2.80 Å for chloride, bromide and iodide, respectively. The bond distances in the chloride and bromide glasses were 0.1 Å shorter than those of the corresponding crystals whereas the bond distance in the iodide glass was the same as that in AgI crystal.

Again the coordination structure of the silver halide-based glasses is discussed on the reference to the structural data of complex crystals containing halogenoargentate polyhedra. Figure 11 shows the plot of the Ag–X bond distance against the coordination number for more than 30 complexes and AgX crystals [9, 20, 21]. In the AgCl-based and the AgBr-based

Table 6. Coordination numbers around Ag$^+$ ion, manner of linkage of AgX$_4$ tetrahedra and Ag–X bond distances in the structure of AgX-based glasses simulated by the MD calculation.

| System | X$^-$ coordination number around Ag$^+$ (%) | | | | | Manner of linkage of AgX$_4$ tetrahedron (%) | | Bond distance (Å) |
	3	4	5	6	Average[a]	Corner-sharing	Edge-sharing	
AgCl	0	16	51	33	5.2	93	7	2.71
AgBr	0	11	62	27	5.2	98	2	2.87
AgI	3	88	8	1	4.1	87	13	2.80

[a] Average coordination number.

(a) CuCl system glass   (b) CuBr system glass   (c) CuI system glass
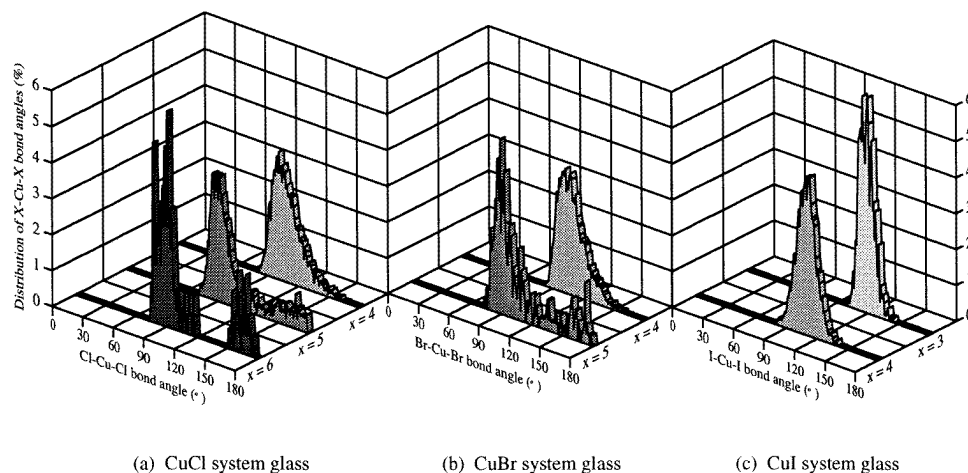
Figure 8. Distribution of X–Cu–X angles (X = Cl, Br, I) in the structure of copper(I) halide-based glasses produced by the MD simulation.

systems, only AgCl and AgBr crystals have sixfold coordination. In the chloroargentate and bromoargentate polyhedra, Ag$^+$ ions are located in coordination sites of fourfold or less than fourfold. For the AgI-based system, the AgI crystal has fourfold coordination at room temperature. Under pressure higher than 4 kbar, however, the AgI crystal has NaCl structure [21]. Other polyhedra in the iodoargentates have coordination of fourfold or less than fourfold. The dependence of the bond distance on the coordination number is similar to that for copper(I) halide compounds although it is not so clear. As seen from figure 11, the bond distance in the AgI-based glass is located in the range of the distance in iodoargentate having fourfold coordination. This is consistent with the coordination number revealed by EXAFS analysis. This is also supported by the MD simulation shown in table 6. In the AgI-based glass, 88% of Ag$^+$ ions are coordinated by four iodide ions. Furthermore, the distribution of the bond angle, I–Ag–I, in the fourfold coordination has a peak around 110°, indicating that the polyhedra are tetrahedral as well as those in the copper(I) halide-based glasses. Therefore, we conclude that the main structural unit in the AgI-based glass is AgI$_4$ tetrahedra.

On the other hand, the bond distances in the AgCl-based and the AgBr-based glasses, which were obtained from EXAFS analyses, are in the range of the bond distance in

(a) AgCl system glass   (b) AgBr system glass   (c) AgI system glass
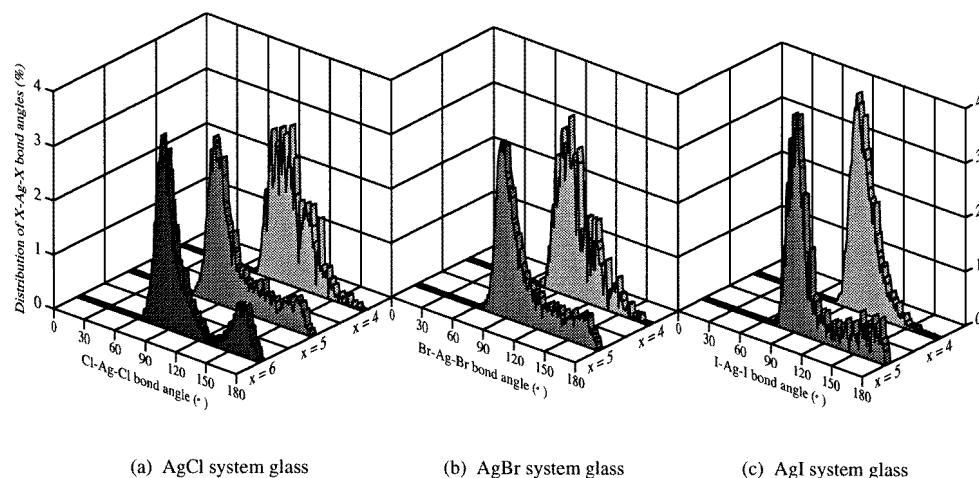
Figure 9. Distribution of X–Ag–X angles (X = Cl, Br, I) in the structure of silver halide-based glasses produced by the MD simulation.

halogenoargentate polyhedra with fourfold coordination. This is inconsistent with the coordination number expected in the EXAFS analyses. In order to discuss this discrepancy, we refer to the results of the MD simulations. The structure of the AgCl-based and the AgBr-based glasses produced by the MD simulations is different from those of the other glasses, i.e., the copper(I) halide-based and the AgI-based glasses. As shown in table 6, silver ions located in fourfold, fivefold and sixfold coordination sites are 16, 51 and 33%, respectively, for the AgCl-based glass and 11, 62 and 27% for the AgBr-based glass. These results suggest that in the AgCl-based and the AgBr-based glasses the coordination numbers of Ag^+ sites are widely distributed and that the average coordination number is higher than four. The wide distribution in the coordination number indicates that the coordination shells in these glasses are largely disordered in comparison with the other glass systems, i.e., the copper halide-based and the AgI-based glasses. The disordered coordination means that the nearest-neighbouring coordination shells are not definitely distinguished from the next-neighbouring ones. Such ill defined coordination shells have also been discussed for LiCl-based, LiBr-based and LiI-based glasses although most Li^+ ions in the lithium halide-based glasses are tetrahedrally coordinated by halide ions [12]. The ill defined local order in the lithium halide-based glasses is attributed to the weak attractive interaction between cations and anions in the 1:1 Coulombic systems. Indeed, in the 4:2 or 2:1 Coulombic systems which have stronger interaction, such as SiO_2, BeF_2 and $ZnCl_2$, the network structure consists of well defined tetrahedral units. The AgCl-based and the AgBr-based glasses are also approximately considered as 1:1 Coulombic systems. Furthermore, we have to also account for the size effect of cation and anion. In a simple model for ionic systems, the cation and anion are regarded as charged hard spheres with ionic radii r_+ and r_- respectively. When the radius ratio, r_+/r_-, is in the range of 0.22 and 0.41, the tetrahedral coordination around the cation is preferred. For the r_+/r_- ratio larger than 0.41 and less than 0.65, the coordination shell becomes sixfold [22]. Applying this model to the silver halide-based systems, we have to know the radii of Ag^+ and halide ions. Assuming that the radii of Cl^- and Br^- are 1.81 and 1.96 Å [23], the radii of Ag^+ in the AgCl-based and the AgBr-based glasses are estimated to be 0.84 and 0.83 Å, respectively, from the difference between the
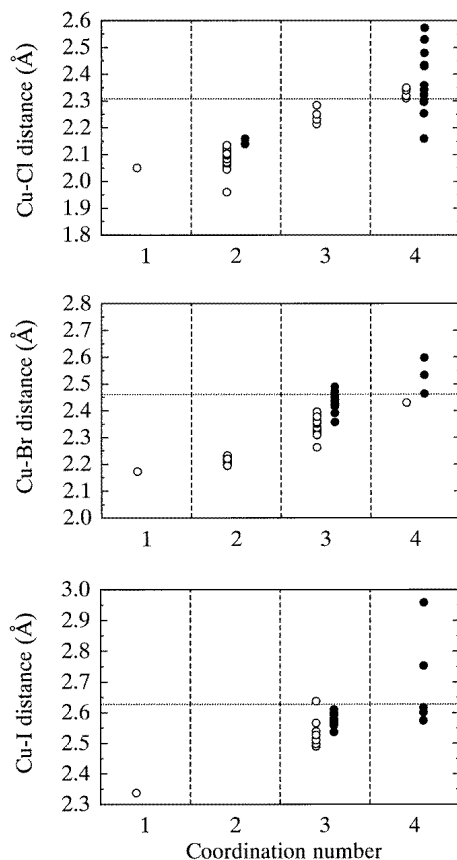
Figure 10. Cu–X bond distances (X = Cl, Br, I) in halogenocuprate(I) polyhedra and CuX crystals against coordination number. Open circles and closed circles are the Cu-*terminal* X and Cu-*bridging* X distances, respectively. The bond distances of the coordination number 1 are those of gas phase CuX. When the bond distances are widely distributed in the same crystal, the maximal and minimal distances are plotted. Horizontal dotted lines indicate Cu–X bond distances in the real glasses obtained by EXAFS analyses.

bond distances and the radii of the anions. Then, r_+/r_- ratios are calculated to be 0.46 and 0.42 for the AgCl-based and the AgBr-based glasses, respectively. These values are on the border between tetrahedral and octahedral coordination. Therefore, the local structures of the AgCl-based and the AgBr-based glasses are probably disordered much more than those of the lithium halide-based glasses.

Although it is difficult to determine the coordination number definitely, the number of the nearest-neighbouring halide ions around Ag^+ should be four or larger than four.

5. Conclusions

The structures of copper(I) halide-based and silver halide-based glasses, AX–MX–M$'$X$_2$ (A = Cu, Ag, M = alkali, M$'$ = alkaline-earth, X = Cl, Br, I) were investigated by means of extended x-ray absorption fine structure spectroscopy (EXAFS) and molecular
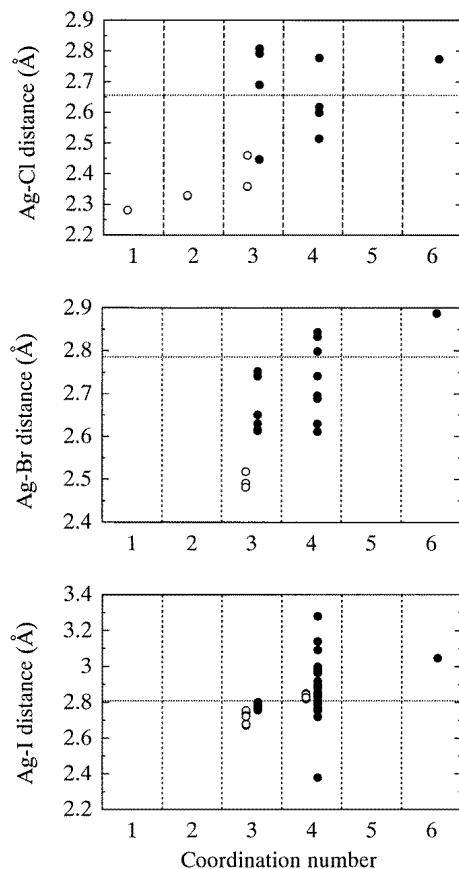
Figure 11. Ag–X bond distances (X = Cl, Br, I) in halogenoargentate polyhedra and AgX crystals against coordination number. Open circles and closed circles are the Ag-*terminal* X and Ag-*bridging* X distances, respectively. The bond distances of the coordination number 1 are those of gas phase AgX. When the bond distances are widely distributed in the same crystal, the maximal and minimal distances are plotted. Horizontal dotted lines indicate Ag–X bond distances in the real glasses obtained by EXAFS analyses.

dynamics (MD) simulation. The main structural units in the copper(I) halide-based and the AgI-based glasses are corner-shared AX_4 tetrahedra. In the AgCl-based and the AgBr-based glasses, on the other hand, the coordination shells are expected to be much disordered and ill defined compared with those in the copper(I) halide-based and the AgI-based glasses. Although the coordination number for the AgCl-based and the AgBr-based glasses cannot be determined clearly, it is anticipated that more than four halide ions are present in the nearest-neighbouring coordination shells of Ag^+ ions.

Acknowledgments

References

[1] Poulain M, Poulain M, Lucas J and Brun P 1975 *Mater. Res. Bull.* **10** 243
[2] For example, Aggarwal I D and Lu G 1991 *Fluoride Glass Fiber Optics* (San Diego, CA: Academic) and references therein
 Kawamoto K, Horisaka H, Hirao K and Soga N 1985 *J. Chem. Phys.* **83** 2398
[3] For example, Lucas J and Adam J-L 1991 *Optical Properties of Glass* ed D R Uhlmann and N J Kreidl (Westerville, OH: American Ceramic Society) pp 44–46 and references therein
 Lucas J and Adam J-L 1991 *Glastech. Ber.* **62** 422 and references therein
 Yamane M, Inoue S and Nakamura A 1982 *J. Physique. Coll.* **9** 239
 Liu C, Sunder H G and Angell C A 1985 *Mater. Res. Bull.* **20** 525
 Ding M F, Lau J and Mackenzie J-D 1986 *J. Non-Cryst. Solids* **80** 538
 Liu C, Sunder H G and Angell C A 1986 *Solid State Ion.* **18/19** 442
 Almeida R M and Santos L F 1989 *J. Am. Ceram. Soc.* **72** 2065
 Lucas J and Zhang X H 1990 *J. Non-Cryst. Solids* **125** 1
[4] Kadono K, Shimomura T, Kinugawa K and Tanaka H 1990 *J. Non-Cryst. Solids* **116** 33
 Kadono K, Shimomura T and Tanaka H 1991 *Phys. Chem. Glasses* **32** 29
[5] Kadono K, Mitani K, Kinugawa K and Tanaka H 1990 *J. Non-Cryst. Solids* **122** 214
 Kadono K, Mitani K, Kinugawa K and Tanaka H 1990 *J. Mater. Sci. Lett.* **9** 21
 Kadono K, Yasuyoshi A, Nakano K, Kinugawa K and Tanaka H 1992 *J. Ceram. Soc. Japan* **100** 233
[6] Kadono K, Kageyama H, Kamijo K and Tanaka H 1992 *J. Non-Cryst. Solids* **140** 98
 Kadono K, Kageyama H, Kamijo K, Kinugawa K and Tanaka H 1993 *Japan. J. Appl. Phys.* **32** 661
[7] Desa J A E, Wright A C, Wong J and Sinclair R N 1982 *J. Non-Cryst. Solids* **51** 57 and references therein
[8] Kadono K, Mitani K, Kawamoto Y, Ohno K and Kanno R 1991 *Phys. Chem. Glasses* **32** 207
 Kadono K, Mitani K, Yamashita M and Tanaka H 1991 *Solid State Ion.* **47** 227
 Kadono K, Mitani K, Yamashita M, Tanaka H, Kawamoto Y, Ohno K and Kanno R 1992 *J. Non-Cryst. Solids* **140** 103
[9] Wells A F 1982 *Structural Inorganic Chemistry* (Oxford: Clarendon) pp 408–12
[10] Ohno H, Yoroki M, Furukawa K, Takagi Y and Nakamura T 1978 *J. Chem. Soc. Faraday Trans.* I **74** 1861
 Ohno H, Furukawa K, Igarashi K and Mochinaga J 1981 *J. Chem. Soc. Faraday Trans.* I **78** 1555
 Howe M A and McGreevy R L 1988 *Phil. Mag.* B **58** 485
 McGreevy R L and Howe M A 1989 *J. Phys.: Condens. Matter* **1** 9957
 Li J-C, Titman J M, Carr G E, Cowlam N and Suck J-B 1989 *Physica* B **156/157** 168
[11] Ohno H, Igarashi K, Umesaki N and Furukawa K 1994 *X-ray Diffraction Analysis of Ionic Liquids* (Aedermannsdorf: Trans Tech)
 Page D I and Mika K 1971 *J. Phys. C: Solid State Phys.* **4** 3034
 Eisenberg S, Jal J-F, Dupuy J, Chieux P and Knoll W 1982 *Phil. Mag.* A **46** 195
 Allen D A and Howe R A 1992 *J. Phys.: Condens. Matter* **4** 6029
 Shirakawa Y, Saito M, Tamaki S, Inui M and Takeda S 1991 *J. Phys. Soc. Japan* **60** 2678
 Inui M, Takeda S, Shirakawa Y, Tamaki S, Waseda Y and Yamaguchi Y 1991 *J. Phys. Soc. Japan* **60** 3025
[12] Kinugawa K, Ohtori N, Kadono K, Tanaka H, Okazaki S, Misawa M and Fukunaga T 1993 *J. Chem. Phys.* **99** 5345
[13] Kinugawa K, Kadono K and Tanaka H 1991 *Computer Aided Innovation of New Materials* ed M Doyama, T Suzuki, J Kihara and R Yamamoto (Elsevier)
 Kinugawa K 1993 *Phys. Rev.* B **48** 10 097
[14] Zachariasen W H 1932 *J. Am. Chem. Soc.* **54** 3841
[15] Kawamura K 1990 *Pasokon Bunshi Shimyureishon—Molecular Simulation by Personal Computers* (Tokyo: Kaibundo)
[16] Sakane H 1991 *PhD Thesis* Osaka University; the main parts of the programs used in these analyses were XASANAL, FTRANS, FFILTER and CFL.
[17] McKale A G, Veal B W, Paulikas A P, Chan S-K and Knapp G S 1988 *J. Am. Chem. Soc.* **110** 3763
[18] Bordiga S, Coluccia S, Lamberti C, Marchese L, Zecchina A, Boscherini F, Buffa F, Genoni F, Leofanti G, Petrini G and Vlaic G 1994 *J. Phys. C: Solid State Phys.* **98** 4125
[19] Andersson S and Jagner S 1985 *Acta Chem. Scand.* A **39** 297
 Andersson S and Jagner S 1985 *Acta Chem. Scand.* A **39** 423
 Andersson S and Jagner S 1985 *Acta Chem. Scand.* A **39** 515
 Andersson S and Jagner S 1985 *Acta Chem. Scand.* A **39** 577
 Andersson S and Jagner S 1985 *Acta Chem. Scand.* A **39** 799

Andersson S and Jagner S 1986 *Acta Chem. Scand.* A **40** 52
Andersson S and Jagner S 1986 *Acta Chem. Scand.* A **40** 177
Andersson S and Jagner S 1986 *Acta Chem. Scand.* A **40** 210
Andersson S and Jagner S 1987 *Acta Chem. Scand.* A **40** 230
Andersson S and Jagner S 1987 *Acta Crystallogr.* C **43** 1089
Andersson S and Jagner S 1988 *Acta Chem. Scand.* A **42** 691
Asplund M and Jagner S 1984 *Acta Chem. Scand.* A **38** 135
Asplund M and Jagner S 1984 *Acta Chem. Scand.* A **38** 297
Asplund M and Jagner S 1984 *Acta Chem. Scand.* A **38** 411
Asplund M and Jagner S 1985 *Acta Chem. Scand.* A **39** 47
Asplund M, Jagner S and Nilsson M 1982 *Acta Chem. Scand.* A **36** 751
Asplund M, Jagner S and Nilsson M 1983 *Acta Chem. Scand.* A **37** 57
Asplund M, Jagner S and Nilsson M 1984 *Acta Chem. Scand.* A **38** 57
Asplund M, Jagner S and Nilsson M 1985 *Acta Chem. Scand.* A **39** 447
Baglio J A and Vaughan P A 1970 *J. Inorg. Nucl. Chem.* **32** 803
Baglio J A, Weakliem H A, Demelio F and Vaughan P A 1970 *J. Inorg. Nucl. Chem.* **32** 795
Bhaduri S, Sapre N Y and Jones P G 1991 *J. Chem. Soc. Dalton Trans.* 2539
Bowmaker G A, Camus A, Skelton B W and White A H 1990 *J. Chem. Soc. Dalton Trans.* 727
Bowmaker G A, Clark G R, Rogers D A, Camus A and Marsich N 1984 *J. Chem. Soc. Dalton Trans.* 37
Bowmaker G A, Clark G R and Yuen D K P 1976 *J. Chem. Soc. Dalton Trans.* 2329
Brink C and MacGillavry C H 1949 *Acta Crystallogr.* **2** 158
Brink C and van Arkel A E 1952 *Acta Crystallogr.* **5** 506
Brink C, Binnendijk N F and van de Linde J 1954 *Acta Crystallogr.* **7** 176
Bu X, Coppens P, Lederle B and Naughton M J 1991 *Acta Crystallogr.* C **47** 2082
Clegg W, Garner C D, Nicholson J R and Raithby P R 1983 *Acta Crystallogr.* C **39** 1007
Fackler J P Jr, López C A and Winpenny R E P 1992 *Acta Crystallogr.* C **48** 2218
Francisco R H P, de Almeida Santos R H, Lechat J R and Massabni A C 1981 *Acta Crystallogr.* B **37** 232
Geiser U, Wang H H, Hammond C E, Firestone M A, Beno M A, Carlson K D, Nuñez L and Williams J M
    1987 *Acta Crystallogr.* C **43** 656
Huber C, Post M L and Siiman O 1978 *Acta Crystallogr.* B **34** 2629
Kaiser J, Brauer G, Schröder F A, Taylor I F and Rasmussen S E 1974 *J. Chem. Soc. Dalton Trans.* 1490
Kawamoto A, Tanaka J and Tanaka M 1987 *Acta Crystallogr.* C **43** 205
Manson E L, De Lucia F C and Gordy W 1975 *J. Chem. Phys.* **62** 1040
Manson E L, De Lucia F C and Gordy W 1975 *J. Chem. Phys.* **62** 4796
Manson E L, De Lucia F C and Gordy W 1975 *J. Chem. Phys.* **63** 2724
Marsh W C and Trotter J 1971 *J. Chem. Soc.* A 1482
Newton M G, Caughman H D and Taylor R C 1970 *J. Chem. Soc. Chem. Commun.* 1227
Newton M G, Caughman H D and Taylor R C 1974 *J. Chem. Dalton Trans.* 258
Scott B and Willett R D 1991 *Acta Crystallogr.* C **47** 1389
Scott B and Willett R D 1991 *Inorg. Chem.* **30** 110
Simonsen O and Toftlunch H 1987 *Acta Crystallogr.* C **43** 831
Tsuboyama S, Kobayashi K, Sakurai T and Tsuboyama K 1984 *Acta Crystallogr.* C **40** 1178
Willett R D 1987 *Inorg. Chem.* **26** 3424
Willett R D and Halvorson K 1988 *Acta Crystallogr.* C **44** 2068
Wong C-H and Schomaker V 1957 *J. Phys. C: Solid State Phys.* **61** 358
[20] Bassett W A and Takahashi T 1965 *Am. Mineral.* **50** 1576
Bowles J C and Hall D 1971 *Acta Crystallogr.* B **31** 2149
Brink C and Kroese S H A 1952 *Acta Crystallogr.* **5** 433
Brown I D, Howard-Lock H E and Natarajan M 1977 *Can J. Chem.* **55** 1511
Coetzer J 1975 *Acta Crystallogr.* B **31** 622
Coetzer J and Thackeray M M 1975 *Acta Crystallogr.* B **31** 2113
Geller S and Lind M D 1970 *J. Chem. Phys.* **52** 5854
Gilmore C J, Tucker P A and Woodward P 1971 *J. Chem. Soc.* A 1337
Helgesson G and Jagner S 1988 *Acta Crystallogr.* C **44** 2059
Helgesson G and Jagner S 1988 *J. Chem. Soc. Dalton Trans.* 2117
Helgesson G and Jagner S 1990 *J. Chem. Soc. Dalton Trans.* 2413
Helgesson G and Jagner S 1991 *Inorg. Chem.* **30** 2574
Helgesson G, Josefsson M and Jagner S 1988 *Acta Crystallogr.* C **44** 1729

Jagner S, Olson S and Stomberg R 1986 *Acta Chem. Scand.* A **40** 230
Jones P G 1992 *Acta Crystallogr.* C **48** 1314
Keller H J, Keppler B and Pritzkow H 1982 *Acta Crystallogr.* B **38** 1603
Krisher L and Norris W 1966 *J. Chem. Phys.* **44** 391
Meyer Von H-J 1963 *Acta Crystallogr.* **16** 788
Peters K, Ott W and von Schnering H G 1982 *Angew. Chem. Int. Edn Engl.* **21** 697
Shoemaker C B 1976 *Acta Crystallogr.* B **32** 1619
Stomberg R 1969 *Acta Chem. Scand.* **23** 3498
Thackeray M M and Coetzer J 1975 *Acta Crystallogr.* B **31** 2339
Thackeray M M and Coetzer J 1975 *Acta Crystallogr.* B **31** 2341
Thackeray M M and Coetzer J 1978 *Acta Crystallogr.* B **34** 71
[21] Moore M J and Kas J S 1968 *J. Chem. Phys.* **48** 2446
[22] Wells A F 1982 *Structural Inorganic Chemistry* 5th edn (Oxford: Clarendon) pp 315–7
[23] Shannon R D and Prewitt C T 1969 *Acta Crystallogr.* B **25** 925